Band Structure and Density of States Effects in Co-Based Magnetic Tunnel Junctions

P. LeClair,[1] J. T. Kohlhepp,[1] C. H. van de Vin,[1] H. Wieldraaijer,[1] H. J. M. Swagten,[1] W. J. M. de Jonge,[1]
A. H. Davis,[2] J. M. MacLaren,[2] J. S. Moodera,[3] and R. Jansen[3,4]

[1]*Department of Applied Physics, Eindhoven University of Technology, P.O. Box 513, 5600 MB Eindhoven, The Netherlands*
[2]*Department of Physics, Tulane University, New Orleans, Louisiana 70118*
[3]*Francis Bitter Magnet Laboratory, Massachusetts Institute of Technology, Cambridge, Massachusetts 02139*
[4]*MESA$^+$ Research Institute, University of Twente, 7500 AE Enschede, The Netherlands*

(Received 4 July 2001; published 20 February 2002)

Utilizing $Co/Al_2O_3/Co$ magnetic tunnel junctions with Co electrodes of different crystalline phases, a clear relationship between electrode crystal structure and junction transport properties is presented. For junctions with one fcc(111) textured and one polycrystalline (polyphase and polydirectional) Co electrode, a strong asymmetry is observed in the magnetotransport properties, while when both electrodes are polycrystalline the magnetotransport is essentially symmetric. These observations are successfully explained within a model based on ballistic tunneling between the calculated band structures (density of states) of fcc-Co and hcp-Co.

DOI: 10.1103/PhysRevLett.88.107201 PACS numbers: 73.40.Gk, 75.70.–i, 85.30.Mn, 85.70.Kh

One of the most basic and essential aspects of magnetic tunnel junctions (MTJs) [1] is the role of the electronic structure in determining MTJ properties. The sensitivity of tunnel current to the electronic structure of the tunneling electrodes has been well established theoretically for some time [2–4]. Experimentally, there have been few conclusive observations of the electronic structure of a *normal* (i.e., not superconducting or a semimetal [5]) metal in tunneling experiments, despite extensive efforts [6–8]. Spin polarized tunneling in superconductor-insulator-ferromagnet junctions [9], for example, can only reveal the spin polarization of the participating density of states (DOS) (at the Fermi level) of electrons tunneling from the ferromagnet. More recently, De Teresa *et al.* [10] have used half-metallic $La_{0.7}Sr_{0.3}MnO_3$ (LSMO) in $Co/SrTiO_3/LSMO$ junctions to analyze the sign and magnitude of the Co spin polarization as a function of bias, pointing out the importance of participating tunneling states. Yuasa *et al.* [11] have also recently shown a dependence of the tunneling spin polarization on crystallographic orientation for epitaxial Fe electrodes. Still, few examples of a clear experimental correlation between the conductance properties and the electronic structure of normal metal electrodes with a clear theoretical analysis have been identified, particularly for magnetic junctions.

The difficulties in observing band structure or density of states effects in normal metal junctions (or MTJs) are numerous. One limitation is that one can only hope to see band or DOS features for those bands that contribute to the tunnel conductance. These bands and the DOS they generate are (for the Al_2O_3 barriers utilized) believed to be limited to highly dispersive bands whose states at finite k are s hybridized [3,4,6,9,12]. A second complication is the presence of many conductance (i.e., dI/dV) contributions, such as normal elastic tunneling and inelastic excitations (phonons, magnons), which may obscure electronic structure features, but which may be essentially eliminated with careful analysis [6]. A third complication is the extreme difficulty in the theoretical analysis of these structures, particularly MTJs. A last, and perhaps most fatal, complication is the need for tunneling electrodes with a *known physical and electronic structure which can be modulated* in order to convincingly compare theory and experiment.

In this Letter, we prepare $Co/Al_2O_3/Co$ MTJs with differently textured Co layers, viz., highly textured fcc(111)-Co and polycrystalline-Co, in order to realize a model system in which to study the relation between electronic and crystal structure and MTJ properties. Using only Co, but in different crystalline phases (and hence with different electronic structure), crucially allows us to focus *only* on changes in the electronic and crystal structure. By a careful analysis of the conductance-voltage (dI/dV-V) and magnetoresistance-voltage characteristics, in combination with ^{59}Co nuclear magnetic resonance (NMR) *to directly investigate local physical structure,* we show experimentally that junctions with electrodes of two different crystalline phases show obviously asymmetric transport characteristics. The observed asymmetries can be qualitatively explained by a model developed by us [13–15] based on ballistic tunneling between the calculated band structures (and resulting DOS) of fcc-Co and hcp-Co. Furthermore, these experimental and theoretical results may explain several related observations of similar conductance asymmetries [8,16–18].

Ferromagnetic tunnel junctions were prepared by UHV dc/rf magnetron sputtering; the details of this fabrication process have been described in [19,20]. The tunnel magnetoresistance (TMR) structures used consisted of $Si(001)/SiO_2$/buffer/Co $d_{Co}/Al_2O_3/Co$ 150 Å/Al 30 Å postannealed in a magnetic field at 200 °C. For these experiments, the buffer was either Ta 50 Å/Co 70 Å/FeMn 100 Å ("FeMn-based buffer") or only Ta 50 Å ("Ta buffer"). Junction resistances or differential resistances

($dV/dI \equiv G^{-1}$, where $dI/dV \equiv G$ is the conductance) were measured using standard *dc* or *ac* lock-in techniques. *In all cases, the bottom electrode was biased positively for $V > 0$.*

In order to prove that Co layers grown on FeMn-based and Ta-based buffers have a different physical structure, we performed ^{59}Co NMR measurements on separately grown Si/SiO_2/Ta 50 Å/Co *d* d_{Co}/Al_2O_3 (Ta-based), Si/SiO2/Ta 50 Å/Cu 70 Å/FeMn 100 Å/Co d_{CO}/Al_2O_3 (FeMn-based), and Al_2O_3/Co 150 Å (to represent the top electrode) structures, sputtered under identical conditions [21]. The NMR experiments were performed at 1.5 K in zero applied field, as described in [22]. NMR measurements give information on the distribution hyperfine fields at the Co nuclei, from which it is possible to distinguish Co atoms in different structural environments (e.g., fcc, hcp, bcc) and to determine their relative amounts [22,23].

Figure 1 shows the resulting ^{59}Co NMR intensity as a function of frequency for FeMn-based structures (Fig. 1a) with $d_{Co} = 35$, 50, 80 Å, Al_2O_3/Co/Al structures with $d_{Co} = 80$ Å, and for a Ta-based structure with $d_{Co} = 50$ Å (Fig. 1b). The vertical lines indicate the frequencies for bulk hcp (magnetization ∥ or ⊥ to the *c* axis) and fcc Co. Focusing on the FeMn-based structures, (Fig. 1a), a strong line is observed at the frequency corresponding to fcc-Co for $d_{Co} = 50$ Å and 80 Å, with little intensity at the hcp-Co positions or intervening regions (corresponding to stacking faults [22,23]). For the 35 Å, the dominant line is still fcc-Co, but considerable intensity exists at the hcp-Co and stacking fault positions. However, from 35-80 Å the stacking fault intensity does not increase. From this, we may conclude that Co growth begins with a considerable amount of stacking faults, but then grows in a more ordered fcc structure, with presumably the purest fcc-Co present at the uppermost surface. Thus, even the 35 Å Co layer has predominantly fcc-Co stacking for the topmost layers adjacent to the barrier. Combining the NMR data with x-ray diffraction measurements indicates that the Co layers with FeMn-based buffers are (111) textured fcc-Co.

Figure 1b shows the NMR intensity spectrum for representative Ta-based and Al_2O_3-based samples. No significant Co thickness dependence was observed, indicating that the growth mode is the same for all thicknesses. For either the Ta-based samples or those grown on Al_2O_3, intensity is observed for both hcp positions as well as the fcc position and all intermediate stacking fault positions. From this, we may conclude that Co grows on Ta or Al_2O_3 in a random, polycrystalline and polyphase manner [22,23] (which we refer to as "poly-Co" for simplicity), in contrast to the fcc(111)-textured Co in FeMn-based structures. Thus, the FeMn-based and Ta-based MTJs prepared for this study may be clearly identified as *asymmetric* fcc(111)-Co/Al_2O_3/poly-Co and *symmetric* poly-Co/Al_2O_3/poly-Co junctions, respectively. We must caution that, although the FeMn-based junctions produce *strongly fcc(111)-textured* bottom electrodes, they contain a fraction of Co atoms which remains in a non-fcc environment.

One may anticipate that these structural differences lead to differences in band structure and DOS, and, hence, differences in transport properties. From symmetry, one expects that a physically asymmetric junction results in transport which is asymmetric with respect to bias. Figure 2a shows the conductance-voltage [$dI/dV(V) \equiv G(V)$] characteristics, normalized at $V = 0$, for parallel Co magnetizations at 5 K for two fcc(111)-Co d_{Co}/Al_2O_3/poly-Co junctions with $d_{Co} = 35, 50$ Å and a poly-Co/Al_2O_3/poly-Co junction. The fcc(111)-Co/Al_2O_3/poly-Co junctions show an obvious conductance asymmetry, with most notably a local minimum at

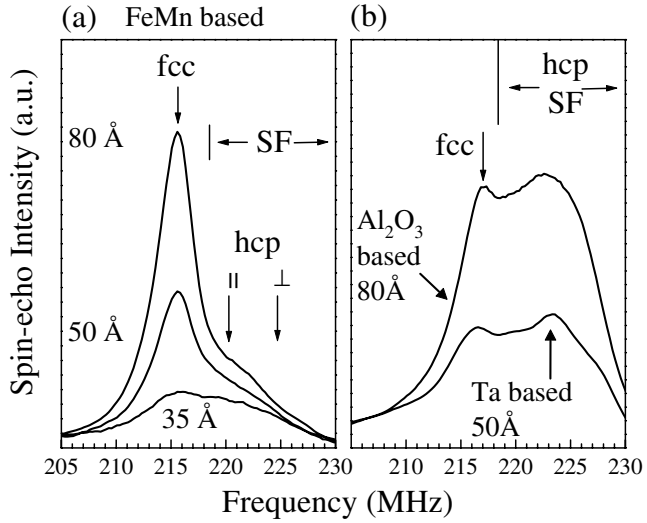

FIG. 1. ^{59}Co NMR spectra at 1.5 K in zero applied field for (a) FeMn-based structures with varying d_{Co} (see text) and (b) Ta/Co/Al_2O_3 and Al_2O_3/Co/Al structures.

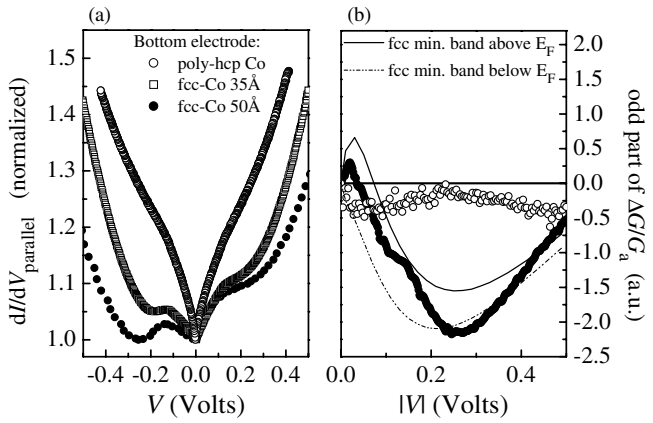

FIG. 2. (a) Conductance-voltage (dI/dV-V) characteristics, normalized at zero bias, for fcc(111)-Co 35 Å, 50 Å/Al_2O_3/poly-Co, and poly-Co/Al_2O_3/poly-Co junctions, for parallel magnetization alignments at 5 K. (b) Odd part of $\Delta G/G_a$ vs voltage. Experimental data at 5 K (points), and calculated curves (lines, ×5) for a fcc-Co/I/hcp-Co junction (see text).

~ -0.25 V and a slight "shoulder" at the same positive voltage, only for parallel magnetizations. Parenthetically, we note that the asymmetry was also present for intentionally over- or underoxidized barriers. We will return to the explanation of these unusual features shortly. The poly-Co/Al_2O_3/poly-Co junctions show almost perfectly symmetric behavior for both magnetization orientations, with a parabolic background and a low-voltage linear contribution, with no apparent thickness dependence. For both types of junctions, the former parabolic portion can be understood in terms of regular elastic tunneling [6], whereas the linear contribution is consistent with magnon-assisted tunneling [16]. However, the local minimum and shoulder observed for fcc(111)-Co/Al_2O_3/poly-Co junctions cannot be explained by either of these mechanisms. The striking difference between junctions where only the crystalline phase of the bottom electrode was intentionally altered suggests that the electronic structure and spin-dependent DOS of the fcc-Co structure must be responsible.

If the DOS and band structure differences between the two Co electrodes are responsible, one may expect the bias dependence of the TMR to be altered as well. Although the TMR was generally lower for poly-Co/Al_2O_3/poly-Co structures, this criterion is very susceptible to slight differences in preparation conditions. The normalized *differential* TMR-voltage [$\Delta G/G_{\mathrm{ap}}(V)$, normalized at $V = 0$] characteristics, though generally nearly identical for many junctions [20], suffer from a strong contribution by inelastic excitations [16] which may mask the underlying electronic structure effects. The main inelastic excitation contribution is due to magnon excitations in the electrodes [16], which give a contribution symmetric in applied bias. If we assume as a rough approximation that the magnon excitation spectra for poly-Co and fcc(111)-Co are similar, by plotting the *odd* part of the differential TMR-voltage behavior, the magnon-assisted conductance contributions cancel, and we may be primarily sensitive to only electronic structure (or self-energy) effects [6]. For any excitations within the barrier (e.g., phonons), this assumption is very well justified [6]. We emphasize that this sort of analysis is *crucial* for comparison with theory, effectively eliminating those contributions which are difficult to incorporate theoretically. Figure 2b shows the odd portion of $\Delta G/G_a$ [i.e., $\Delta G/G_{\mathrm{ap}}(V > 0) - \Delta G/G_{\mathrm{ap}}(V < 0)$] as a function of voltage, a measure of the asymmetry in the bias dependence of the *differential* TMR, $\Delta G/G_{\mathrm{ap}}$ [24]. For poly-Co/Al_2O_3/poly-Co junctions, almost no asymmetry is present, as expected for nominally identical electrodes. However, for fcc(111)-Co/Al_2O_3/poly-Co junctions, there is an obvious strong minimum, corresponding to the same voltage where the local minimum and shoulder features were seen in the $dI/dV(V)$ curves. This further suggests that the electrode DOS and band structure may play a key role. Since the differential TMR more strongly *decreases* at the position of the shoulder and local minimum, one expects that either the minority DOS increases or the majority DOS decreases. As we will show, the dip and shoulder features found in $dI/dV(V)$ can be accounted for theoretically by a combination of band structure and DOS arguments, incorporated into a ballistic model of tunneling [13–15].

The key input for the model used [13–15] is the spin-resolved DOS of the electrodes. The calculated DOS for fcc-Co [13] shows that the total DOS is negatively polarized at E_F, but that the s-DOS is positively polarized. This suggests that states with s character dominate the tunneling with these barriers [4,9,12]. Calculations by us show that the most dispersive bands, corresponding to those which have previously been identified as the source of the tunneling conductance, exhibit significant s hybridization. Since these are hybridized states, every contribution to the s character of the band is accompanied by a contribution to the d character from the same state (and, to a smaller extent, the p character). For Fe, Co, and Ni, in each case there is only a single band with significant s character near E_F. Therefore, the s-DOS emerges as a good marker for the behavior of the conductance (dI/dV) in this bias range. To obtain the s-hybridized partial DOS, the DOS and band structures have been calculated with the layer-KKR (Korringa-Kohn-Rostoker) method [25]. For simplicity, we use hcp(0001) bands to model the poly-Co electrode, since we are looking primarily at features of the fcc DOS, and the hcp s-hybridized bands are relatively featureless in any case. Although it has been previously shown that tunneling is extremely interface sensitive [19,26], we expect that the Co band structure and DOS at the barrier interface, though certainly altered, will strongly resemble the bulk, at least with regard to the general features one may observe [27].

We first observe that the fcc(111) DOS for states with s character above and below E_F has several key features which may explain the underlying tendency for dI/dV to dip in fcc(111)-Co/Al_2O_3/poly-Co junctions. The fcc-Co s-DOS is known to exhibit two sharp peaks at about 0.4 eV above *and* below E_F [13]. DOS peaks imply localized states that have a reduced tunneling probability [9,12,13], and, hence, a smaller contribution to the conductance. For the fcc(111)-Co/Al_2O_3/poly-Co structures, note that in the experimental configuration electrons flow from hcp to fcc bands for positive bias, and fcc to hcp bands for negative bias. For negative bias, tunneling *into the poly-Co electrode,* biasing includes *occupied* states from *below* E_F in the fcc electrode. Since the fcc states below E_F are increasingly localized as bias increases toward 0.4 eV, dI/dV is suppressed, resulting in a dI/dV dip. For tunneling *into the fcc electrode* at positive bias, we expect the same tendency of dI/dV to decrease, because now the similarly localized states *above* E_F are participating. However, for positive bias, an additional effect enters the picture. In the fcc-Co band structure, there is an unoccupied, but very dispersive, minority band which begins just above E_F [13]. Since it is *above* E_F, it only

participates for tunneling *into* the fcc-Co electrode *from* the poly-Co electrode (positive bias). This highly dispersive band contributes spin down states, thus decreasing the TMR, but augmenting dI/dV, since it leads to an overall increase in available states. The emergence of this band thus partially suppresses the tendency of dI/dV to dip for $V > 0$. As a result, the dip for positive bias in dI/dV appears as a shoulder. Since this band participates only for positive bias, it suppresses the TMR only for positive bias, leading to a minimum in the odd part of the differential TMR. Interestingly, earlier work with Cu dusted MTJs [19,20] showed that dusting of the fcc electrode suppresses the dip in dI/dV, which in hindsight may further indicate that the dips are fcc-Co specific features.

Figure 2b shows the odd part of the differential TMR *calculated* for a fcc-Co/I/hcp-Co MTJ using the model described in Refs. [14,15]. For the poly-Co/I/fcc-Co structure, the small peak at small biases comes from the aforementioned minority fcc-Co band beginning just above E_F. When this minority fcc-Co band is artificially shifted to begin *below* E_F instead of *above* E_F, the small peak disappears. Thus, appearance of the minority band beginning just above E_F in fcc-Co is clearly responsible for this feature. The overall tendency for the odd part of the differential TMR to increase at low biases is sharply suppressed when this minority band emerges for slightly larger biases. Since the appearance of this band strongly increases the contribution of minority states, the odd part of the differential TMR therefore decreases. Thus, the small peak in the odd part of the TMR is *directly related to the unoccupied minority band of the fcc-Co structure,* and the localized part of the fcc-Co s-DOS is responsible for the deep minimum in the odd part of the differential TMR *and* the tendency of dI/dV to dip at $|V| \sim 0.25$ V. Although the qualitative agreement is excellent, the quantitative agreement is not—calculated values are roughly a factor 5 too small (see Fig. 2b)—probably due to the neglect of conductance contributions which are not symmetric in bias (e.g., differing magnon spectra in the two electrodes) and the relative simplicity of the model used. However, this is as yet a common problem when modeling MTJs. We note parenthetically that the calculated bias dependence for hcp-Co/I/hcp-Co junctions is completely symmetric, and the odd part of the differential TMR is thus identically zero. The small experimentally observed odd part for the poly-Co/I/poly-Co junctions, which resembles that of the poly-Co/I/fcc-Co junction, is probably due to the fact that the poly-Co electrodes contain some fcc(111) crystallites, and in slightly different amounts for the top and bottom electrodes. Finally, we note that these results may explain several similar observations in literature [8,17,18].

In conclusion, we have shown a clear relation between the electronic and physical structure of the magnetic electrodes and the magnetotransport properties of MTJs. The asymmetric magnetotransport properties may be understood by considering the itinerant electron bands in the two crystalline phases of Co, as determined from first-principles calculations, and incorporated into a model of ballistic tunneling.

P. LeClair is supported by the Netherlands technology foundation STW, and work at Tulane was supported by DARPA Grant No. MDA 972-97-1-003.

[1] J. S. Moodera, L. R. Kinder, T. M. Wong, and R. Meservey, Phys. Rev. Lett. **74**, 3273 (1995).
[2] J. A. Appelbaum and W. F. Brinkman, Phys. Rev. **186**, 464 (1969).
[3] S. Zhang and P. M. Levy, Eur. Phys. J. B **10**, 599 (1999).
[4] I. I. Oleinik, E. Y. Tsymbal, and D. G. Pettifor, Phys. Rev. B **62**, 3952 (2000).
[5] A. I. Khachaturov, A. A. Galkin, E. Hatta, and V. M. Svistunov, Low Temp. Phys. **26**, 827 (2000).
[6] E. L. Wolf in *Principles of Electron Tunneling Spectroscopy,* (Oxford University Press, London, 1985), Chap. 8.
[7] R. C. Jaklevic and J. Lambe, Surf. Sci. **37**, 922 (1973).
[8] J. M. Rowell, J. Appl. Phys. **40**, 1211 (1969).
[9] R. Meservey and P. M. Tedrow, Phys. Rep. **238**, 173 (1994).
[10] J. M. D. Teresa *et al.,* Science **286**, 507 (1999).
[11] S. Yuasa *et al.,* Europhys. Lett. **52**, 344 (2000).
[12] W. H. Butler, X. G. Zhang, T. C. Schulthess, and J. M. MacLaren, Phys. Rev. B **63**, 054416 (2001).
[13] A. Davis, Ph. D. thesis, (Tulane University, New Orleans, LA, 2000).
[14] A. H. Davis, J. M. MacLaren, and P. LeClair, J. Appl. Phys. **89**, 7567 (2001).
[15] A. H. Davis and J. M. MacLaren, J. Appl. Phys. **87**, 5224 (2000).
[16] S. Zhang, P. M. Levy, A. C. Marley, and S. S. P. Parkin, Phys. Rev. Lett. **79**, 3744 (1997).
[17] J. S. Moodera, J. Nowak, and R. J. M. van de Veerdonk, Phys. Rev. Lett. **80**, 2941 (1998).
[18] W. Oepts *et al.,* J. Appl. Phys. **89**, 8038 (2001).
[19] P. LeClair *et al.,* Phys. Rev. Lett. **84**, 2933 (2000).
[20] P. LeClair *et al.,* Appl. Phys. Lett. **76**, 3783 (2000).
[21] In this case, a Cu layer was used rather than Co as a polycrystalline seed layer for the FeMn layer, but this has no effect on the resulting texture.
[22] W. J. M. de Jonge, H. A. M. de Gronckel, and K. Kopinga, in *Ultrathin Magnetic Structures II,* edited by B. Heinrich and J. A. C. Bland (Springer-Verlag, Berlin, 1994), p. 279.
[23] P. C. Riedi, T. Thomson, and G. J. Tomka, in *Handbook of Magnetic Materials,* edited by K. H. J. Buschow (Elsevier, Amsterdam, 1999), Vol. 12, pp. 97–258.
[24] This is *not* the same as $\Delta R/R_p$ for finite bias.
[25] J. M. MacLaren *et al.,* Comput. Phys. Commun. **60**, 365 (1990).
[26] P. LeClair *et al.,* Phys. Rev. Lett. **86**, 1066 (2001).
[27] We expect interface states to be localized, and, hence, not contribute significantly to the tunnel current.